Rev. Adv. Mater. Sci. 43 (2015) 77-82

GIANT PLASTICITY OF ULTRANARROW GRAPHENE NANORIBBONS

A.S. Kochnev[1,2] and I. A. Ovid'ko[1,2,3]

[1]Peter the Great St. Petersburg Polytechnic University, St. Petersburg 195251, Russia
[2]St. Petersburg State University, St. Petersburg 198504, Russia
[3]Institute of Problems of Mechanical Engineering, Russian Academy of Sciences, St. Petersburg 199178, Russia

Received: October 29, 2015

Abstract. With molecular dynamics simulations, deformation and fracture processes in ultranarrow graphene nanoribbons are examined. It is revealed that twisted and flat graphene nanoribbons having width of 4 atomic cells exhibit giant plasticity specified by plastic strain degrees of ≈180% and ≈290%, respectively. Such extremely high strain values were never observed in previous experiments and simulations. Plastic deformation of the graphene nanoribbons occurs through generation and re-arrangement of disclinations (non-six membered rings of carbon atoms) as well as transformations of disclinated graphene regions into monatomic carbon chains. Complete failure of the ultranarrow graphene nanoribbons is realized through breaks of C-C interatomic bonds at monatomic carbon chains characterized by high tensile strength of ≈45-50 GPa.

1. INTRODUCTION

Graphene shows the remarkable electronic, thermal, and mechanical properties [1-10], opening up a range of new applications. In particular, graphene exhibits the excellent electronic properties due to its 2D hexagonal crystal structure and the presence of charge carriers behaving like massless particles [1,4]. One of the most effective approaches to modify, design and control the electronic properties of graphene is to fabricate it in the form of nanoribbons, (either flat or twisted) narrow graphene ribbons with widths less than 20 nm [11-15]. In doing so, effects of free edges come into play in graphene nanoribbons (GNRs) and strongly affect their properties. For instance, following theoretical predictions [16-18], the edge effects can control whether a GNR is metallic, insulating or semiconducting. In these circumstances, GNRs with their outstanding electronic properties are viewed as basic elements for a new generation of nanoelectronic devices and nano-electromechanical systems.

Also, graphene shows the unique mechanical properties [5,7,19-21] which are of crucial technological importance. So, following experimental data [19], pristine graphene sheets/membranes are specified by highest ever measured strength (≈ 130 GPa), high elasticity (with maximum elastic strain ≈25%) and superior Young modulus (≈1.0 TPa). At the same time, in most cases, monolayer graphene under mechanical load exhibits a brittle behavior (see, e.g., experimental data [19-21]) that significantly limits its practical utility. Such a behavior involves an elastic deformation stage followed by fast catastrophic failure without plastic deformation capable of preventing dangerously fast fracture processes. In the context discussed, from both fundamental and applied viewpoints it is highly interesting to understand, if one can avoid an undesired brittle behavior of graphene through its manipulations. In this paper,

Corresponding author: I.A. Ovid'ko, e-mail: ovidko@nano.ipme.com

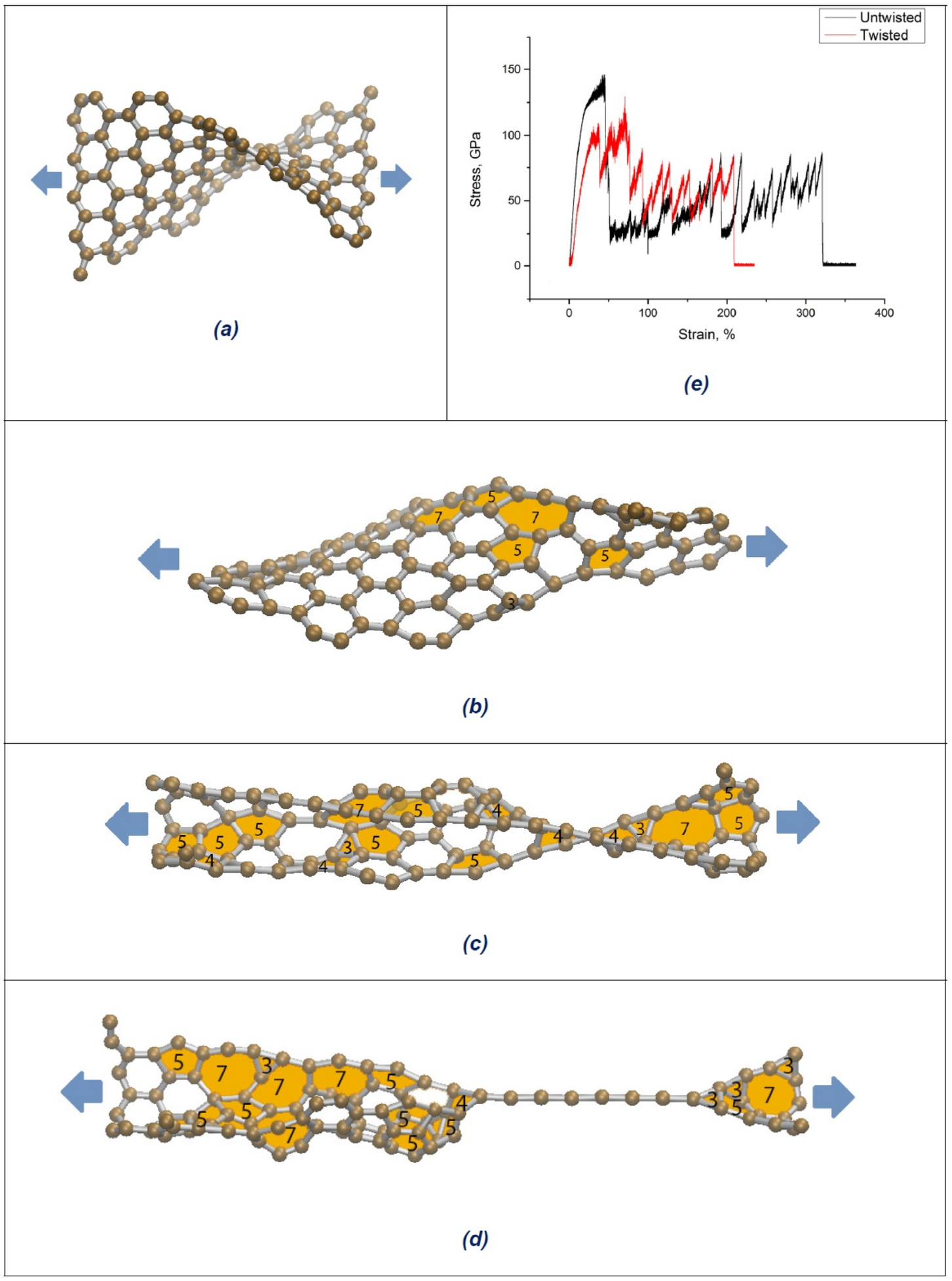

Fig. 1. (Color online) (a) Initial state of twisted graphene nanoribbon. (b)-(d) Structural transformations of twisted graphene nanoribbon during its plastic deformation at strain degrees of (b) $\varepsilon = 40\%$; (c) $\varepsilon = 90\%$; and (d) $\varepsilon = 145\%$. Disclinations - non-six-membered rings of carbon atoms – are yellow colored. Number of ring edges is shown at each disclination. (e) Stress-strain dependences for twisted and flat graphene nanoribbons (red and black curves, respectively) each having width of 4 atomic cells.

with molecular dynamics (MD) simulations, we reveal that graphene in its special geometric form – ultranarrow GNRs – is not brittle and, more than that, shows giant plasticity characterized by plastic strain degrees up to ≈290% prior to failure.

2. RESULTS AND DISCUSSION

In this paper, we consider deformation behaviors of ultranarrow GNRs with width of 4 atomic cells in uniaxial tension tests. In our MD simulations, initially twisted and flat, ultranarrow GNRs (Fig. 1a) under tensile loading are examined (Figs. 1b-1d). In general, GNRs with widths less than 20 nm show the unique electronic and mechanical properties [9-18,22] which are different from those exhibited by large-area graphene due to the edge effects occurring in GNRs. Besides, the non-flat geometry can cause additional effects on the properties of twisted GNRs, by analogy with curved graphene and other carbon materials [23-28]. In the context discussed, it is logical to expect that in the limiting case where flat and twisted GNRs have an ultrasmall width (4 carbon atomic cells), they can exhibit unusual deformation behavior.

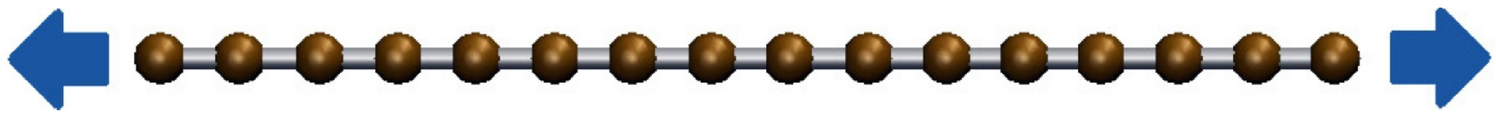

Fig. 2. (Color online) Monatomic carbon chain having 16 atoms under tension along chain axis.

In description of deformation and fracture processes in HDG, we used the Large-scale Atomic/Molecular Massively Parallel Simulator MD simulation package. In order to specify interatomic bonds, the adaptive intermolecular reactive bond order (AIREBO) potential [29] is utilized which is conventionally exploited in computer models of deformation and fracture processes in graphene materials. More details of the computational procedure can be found in Appendix and paper [30].

With MD simulations, we calculated stress-strain dependences for the flat and twisted, ultranarrow GNRs (Fig. 1e). Each of the dependences has the three segments corresponding to elastic straining, plastic deformation and fracture. During an extended plastic deformation (characterized by strain ε ranging from $\approx$30% to $\approx$210% (Fig. 1e)), first, disclinations (non-six membered rings of carbon atoms) are intensively generated in the twisted GNR (Figs. 1 b and 1c). Then, formation of a monatomic carbon chain occurs which joins two separate 2D pieces of the GNR (Fig. 1d). Similar processes come into play in the flat ultranarrow GNR.

The plastic strain degrees, ε_1 ($\approx$180%) and ε_2 ($\approx$290%), exhibited by the twisted and flat GNRs (Fig. 1e), respectively, are really giant. Such extraordinarily high values were never reported in previous experiments and simulations concerning graphene structures.

During plastic deformation, values of the flow stresses σ for the flat and twisted GNRs are in the ranges 20-70 GPa and 35-90 GPa, respectively (Fig. 1e). These values are very high, but they are lower than the experimentally measured [17] intrinsic strength ($\approx$130 GPa) of brittle, micron-sized graphene membrane. Thus, plasticity/ductility of ultranarrow GNRs is enormously enhanced at the expense of a moderate degradation of their strength, as compared to micron-sized graphene.

Also, with MD methods, we simulated tensile tests for isolated monatomic carbon chains (Fig. 2). According to our simulations, tensile strength of a monatomic carbon chain has values of 50, 48 and 45 GPa, when the chain consists of 4, 8, and 16 atoms, respectively. That is, monatomic carbon chains show the “longer is weaker” trend, in which case their elongation makes ultranarrow GNRs (Fig. 1d) weaker during plastic deformation. As a corollary, a monatomic chain can play the role of a “weak point” whose strength controls the fracture strength of the GNR.

Figs. 1a-1d illustrate structural transformations of the twisted GNR during its plastic deformation. The onset of plastic deformation in initially hexagonal crystal lattice of the GNR (Fig. 1a) occurs through generation of dipoles of 5- and 7-disclinations (5- and 7-membered rings of carbon atoms) (Fig. 1b). Such disclination dipoles are equivalent to dislocations [6] that serve as carriers of plastic flow in graphene [31,32]. At the intermediate stage of plastic deformation, new *n*-disclinations (with *n* being 3, 4, 5, and 7) are intensively generated in GNR and form complicated configurations (Fig. 1c).

Note that point n-disclinations in 2D graphene serve as analogues of line disclinations in conventional 3D materials where these line disclinations significantly contribute to plastic deformation at certain conditions. In particular, dipoles and other configurations of line disclinations effectively carry plastic flow in nanocrystalline 3D materials [33-36], and this is called the disclination deformation mechanism. In the context discussed, it is logical to think that dipoles and other configurations of n-disclinations generated at the plastic deformation stage carry plastic flow in 2D graphene materials, including ultranarrow GNRs. This statement is well consistent with the experimental observations [31,32] of plastic deformation carried by dipoles of 5- and 7-disclinations (dislocations) in graphene as well as our simulations (Figs. 1b-1d) demonstrating that n-disclinations are intensively generated and undergo various transformations during plastic deformation of the twisted GNR.

The specific feature of ultranarrow GNRs is in the fact that generation of disclinations is significantly enhanced in them, as compared to conventional GNRs and large-area graphene. The reason is in the effect of GNR free edges that effectively screen stresses of disclinations and thereby dramatically reduce their formation energy $\propto d^2$, where d is the distance between a disclination and the nearest GNR edge. As a corollary, plastic deformation carried by disclinations is facilitated in ultranarrow GNRs specified by extraordinarily small values of d, and such GNRs can exhibit giant plasticity.

It is interesting to notice that disclinations also serve as inevitable structural elements of amorphous graphene [37,38]. In particular, formation and growth of the amorphous phase in graphene under irradiation are identified as generation and expansion of disclination clusters, respectively [37,38]. In the context discussed, we conclude that the disclination mechanism of giant plastic deformation involves local amorphization (Fig. 1c) in ultranarrow GNRs.

With further tension of the initially twisted GNR, one of its disclinated regions is transformed into a monatomic carbon chain (Fig. 1d). Elongation of the chain occurs through both accession of new atoms to it and associated transformations of disclinations in adjacent GNR regions. Thus, at the final stage of plastic deformation, the chain elongation and re-arrangements of disclinations crucially contribute to plastic flow of the ultranarrow GNR. In doing so, the transformations of disclinations are highly enhanced in ultranarrow GNRs due to the pronounced edge effects. The plastic deformation stage in the GNR is followed by its complete failure (separation of the GNR into two isolated pieces) realized via break of an interatomic bond at the monatomic carbon chain.

Note that, following computer simulations [39], the melting of graphene involves intensive formation of dipoles of 5- and 7-discinations as well as transformations of disclinated graphene regions into a 3D network of entangled monatomic carbon chains. These melting mechanisms are similar to physical mechanisms of giant plastic deformation of ultranarrow GNRs, namely stress-induced formation of disclinations (with dominant formation of dipoles of 5- and 7-discinations; see Figs. 1c and 1d) and transformation of disclinated graphene regions into a monatomic carbon chain (Fig. 1d). Thus, there is some similarity between the melting and giant plastic deformation processes in graphene, including, first of all, transformation of 2D graphene structures to 1D carbon chains.

3. CONCLUDING REMARKS

To summarize, following our computer simulations, graphene in its special geometric form – ultranarrow GNRs – exhibits both giant plasticity (specified by superior degrees of plastic strain up to ≈270%) and very high flow stresses (20-90 GPa) (Fig. 1e). Plastic deformation of twisted and flat, ultranarrow GNRs occurs through generation and re-arrangements of disclinations as well as transformations of disclinated graphene regions into a monatomic carbon chain that elongates with rising strain (Figs. 1a-1d). These processes are enhanced in ultranarrow GNRs due to the pronounced effects of free edges that effectively screen stress fields of disclinations and thereby reduce energies specifying their formation and transformations. At the final stage of plastic deformation, a monatomic carbon chain is produced (Fig. 1d) which has a very high tensile strength of ≈45-50 GPa. That is, giant plastic deformation of an ultranarrow graphene nanoribbon involves transformation of 2D graphene structure to 1D carbon chain. According to our simulations, monatomic carbon chains (Fig. 2) show the "longer is weaker" trend, in which case their elongation makes ultranarrow GNRs (Fig. 1d) weaker during plastic deformation. As a consequence, the strength of a monatomic carbon chain (Fig. 1d) controls the fracture strength of the GNR whose complete failure is realized via break of an interatomic bond at the chain. These results are important for understanding the nature of deformation and fracture processes in graphene and other 2D materials.

APPENDIX

A1. General Simulation Method

In simulations of deformation behaviors exhibited by monatomic carbon chains, twisted and flat GNRs, we exploited the Large-scale Atomic/Molecular Massively Parallel Simulator (LAMMPS), a MD simulation package. In order to specify interatomic bonds, we used the adaptive intermolecular reactive bond order (AIREBO) potential [29] conventionally utilized in computer models of graphene structures and their transformations under mechanical load. In our simulations with the AIREBO potential, the cut-off radius specifying short-range covalent interactions is chosen as 2.0 Å.

In order to describe the deformation behavior of GNRs, 3D simulation cells are used with sizes chosen as 20x24x20 $Å^3$. The distance between carbon atoms in graphene in its initial (pre-deformation) state is taken as 1.42 Å. In doing so, the simulation cell contains 100 atoms arranged in 4x10 hexagonal carbon rings of a GNR (Fig. 1a).

Before the computer simulation of tensile deformation of graphene, we performed preprocessing to involve NPT simulation (dynamics with constant pressure and constant temperature) during 100 picoseconds at room temperature and zero pressure at boundaries of the simulation cell. Then the tensile strain was applied along the nanoribbon long axis with a strain rate of 0.05% per picosecond. The simulations were performed at temperature of 300K.

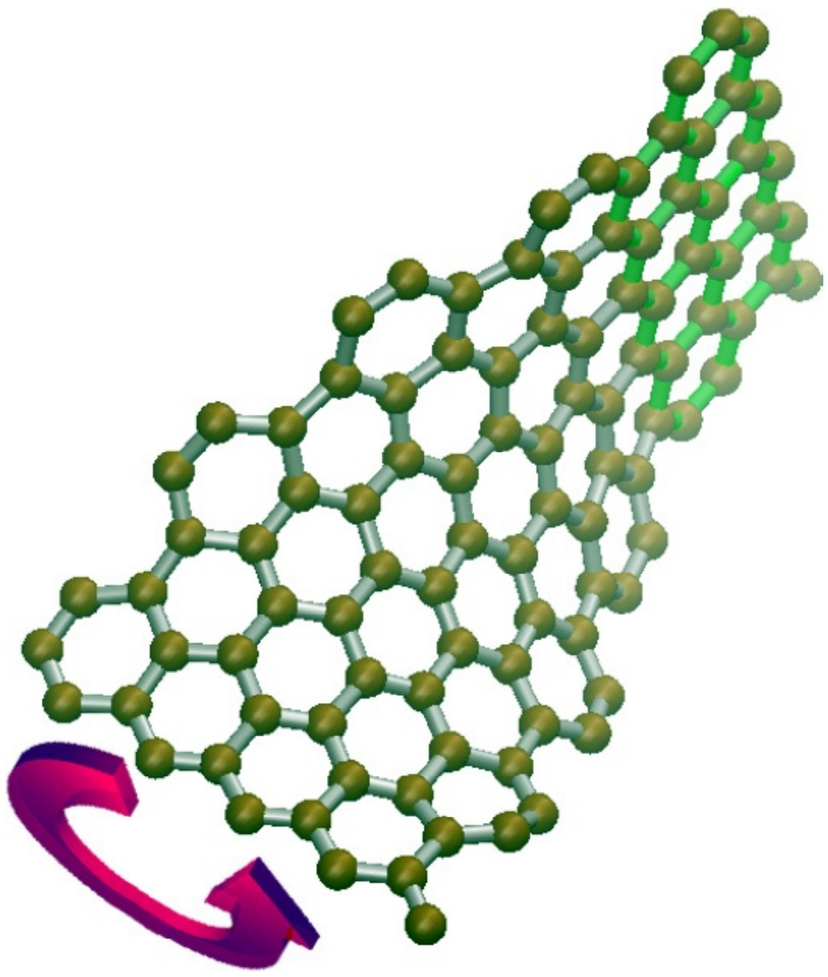

Fig. 3. (Color online) Intermediate stage of simulated twisting transformation of ultranarrow graphene nanoribbon.

A2. Simulations of tensile tests for monatomic carbon chains

Deformation and fracture processes in monatomic carbon chains under tension (Fig. 2) were simulated in order to find characteristic values of their ultimate tensile strength. The tension test was characterized by rate of 0.01 fsec^{-1} in MD simulations with the AIREBO potential exploiting parameters specified for our simulations of flat and twisted nanoribbons (see previous subsection). We examined three monatomic carbon chains consisting of 4, 8, and 16 atoms with chain lengths of 7, 14, and 29 Å, respectively. The simulated chain strength has values of 45, 48, and 50 GPa when the chain contains 16, 8, and 4 atoms, respectively.

A3. Simulations of twisted structure of graphene nanoribbons

In order to form a twisted GNR, we simulate the twisting transformation of a flat GNR. In doing so, first, a region of the initially flat nanoribbon is immobilized which is adjacent to the upper nanoribbon edge and occupies 20% of the nanoribbon area (Fig. 3). (The region in question is green colored in Fig. 3.) A region adjacent to the bottom nanoribbon edge is rotated by 180° around the central axis of the nanoribbon (Fig. 3). The rotation process is simulated, with thermal vibrations of carbon atoms at temperature of T = 100K taken into account. After the rotation process, immobilization of the region adjacent to the left nanoribbon is "switched off", and thermal vibrations again are simulated in the GNR in order to reach its smooth geometric shape. As a result, the twisted GNR is formed (Fig. 1a).

ACKNOWLEDGEMENTS

This work was supported by the Russian Science Foundation (Project 14-29-00199). The simulations were performed at Resource Center "Simulation Center of St. Petersburg State University".

REFERENCES

[1] A.H. Castro Nero, F. Guinea, N.M.R. Peres, K.S. Novoselov and A.K. Geim // *Rev. Mod. Phys.* **81** (2009) 109.
[2] A.A. Balandin // *Nature Mater.* **10** (2011) 569.
[3] I.A. Ovid'ko // *Rev. Adv. Mater. Sci.* **30** (2012) 201.
[4] K.S. Novoselov, V.I. Fal'ko, L. Colombo, P.R. Gellert, M.G. Schwab and K. Kim // *Nature* **490** (2012) 192.
[5] I.A. Ovid'ko // *Rev. Adv. Mater. Sci.* **34** (2013) 1.
[6] O.V. Yazyev and Y.P. Chen // *Nature Nanotechnol.* **9** (2014) 755.
[7] C. Daniels, A. Horning, A. Phillips, D.V.P. Massote, L. Liang, Z. Bullard, B.G. Sumpter and V. Meunier // *J. Phys.: Condens. Matter* **27** (2015) 373002.
[8] J.-W. Jiang, B.-S. Wang, J.-S. Wang and H.S. Park // *J. Phys.: Condens. Matter* **27** (2015) 083001.
[9] J. Lu, Y. Bao, C.L. Su, K.P. Loh, K.P. // *ACS Nano* **7** (2013) 8357.
[10] R. Raccichini, A. Varzi, S. Passerini, B. Scorsati // *Nature Mater.* **14** (2015) 271.
[11] X. Li, X. Wang, L. Zhang, S. Leeand H. Dai // *Science* **319** (2008) 1229.
[12] K.A. Ritter and J.W. Lyding // *Nature Mater.* **8** (2009) 235.
[13] J. Cai, P. Ruffieux, R. Jaafar, M. Bieri, T. Braun, S. Blankenburg, M. Muoth, A.P. Seitsonen, M. Saleh, X. Feng, K. Müllen and R. Fasel // *Nature* **466** (2010) 470.
[14] A. Chuvilin, E. Bichoutskaia, M.C. Gimenez-Lopez, T.W. Chamberlain, G.A. Rance, N. Kuganathan, J. Biskupek, U. Kaiser and A.N. Khlobystov // *Nature Mater.* **10** (2011) 687.
[15] Thomas W. Chamberlain, Johannes Biskupek, Graham A. Rance, Andrey Chuvilin, Thomas J. Alexander, Elena

Bichoutskaia, Ute Kaiser and Andrei N. Khlobystov // *ACS Nano* **6** (2012) 3943.
[16] Y.-W. Son, M.L. Cohen and S. Louie // *Phys. Rev. Lett.* **97** (2006) 216803.
[17] V. Barone, O. Hod and G.E. Scuseria // *Nano Lett.* **6** (2006) 2748.
[18] S. Dutta, S. Lakshmi and S.K. Pati // *Phys. Rev*. *B* **77** (2008) 073412.
[19] C. Lee, X. Wei, J.W. Kysar and J. Hone // *Science* **321** (2008) 385.
[20] Gwan-Hyoung Lee, Ryan C. Cooper, Sung Joo An, Sunwoo Lee, Arend van der Zande, Nicholas Petrone, Alexandra G. Hammerberg, Changgu Lee, Bryan Crawford, Warren Oliver, Jeffrey W. Kysar and James Hone // *Science* **340** (2013) 1073.
[21] J.-H. Lee, P.E. Loya, J. Lou and E.L. Thomas, // *Science* **346** (2014) 1092.
[22] A.V. Orlov and I.A. Ovid'ko // *Rev. Adv. Mater. Sci.* **40** (2015) 249.
[23] M.A.H. Vozmediano, M.I. Katsnelson and F. Guinea // *Phys. Rep.* **496** (2010) 109.
[24] F. Guinea, M.I. Katsnelson and A.K. Geim // *Nature Phys.* **6** (2010) 30.
[25] N. Levy, S.A. Burke, K.L. Meaker, M. Panlasigui, A. Zettl, F. Guinea, A.H. Castro Neto and M.F. Grommie // *Science* **329** (2010) 544.
[26] J. Zabel, R.R. Nair, A. Ott, T. Georgiou, A.K. Geim, K.S. Novoselov and C. Casiraghi // *Nano Lett.* **12** (2011) 617.
[27] V. Atanasov and A. Saxena // *J. Phys.: Condens. Matter*. **23** (2011) 175301.
[28] S. Gupta and A. Saxena // *J. Appl. Phys.* **109** (2011) 074316.
[29] S.J. Stuart, A.B. Tutein and J.A. Harrison // *J. Chem. Phys.* **112** (2000) 6472.
[30] A.S. Kochnev, I.A. Ovid'ko and B.N. Semenov // *Rev. Adv. Mater. Sci.* **37** (2014) 105.
[31] J.H. Warner, E.R. Margine, M. Mukai, A.W. Robertson, F. Giustino and AI. Kirkland // *Science* **337** (2012) 209.
[32] O. Lehtinen, S. Kurasch, A.V. Krasheninnikov and U. Kaiser // Nature Comm. **4** (2013) 2098.
[33] I.A. Ovid'ko // *Science* **295** (2002) 2396.
[34] M. Murayama, J.M. Howe, H. Hidaka and S. Takaki // *Science* **295** (2002) 2433.
[35] C.C. Koch, I.A. Ovid'ko, S. Seal and S. Veprek, *Structural Nanocrystalline Materials: Fundamentals and Applications* (Cambridge University Press: Cambridge, 2007)
[36] S.V. Bobylev, N.F. Morozov and I.A. Ovid'ko // *Phys. Rev. Lett*. **105** (2010) 055504.
[37] F.R. Eder, J. Kotakoski, U. Kaiser and J.C. Meyer // *Sci. Rep*. **4** (2014) 4060.
[38] R. Zhao, J. Zhuang, Z. Liang, T. Yang and F. Ding // *Nanoscale* **7** (2015) 8315.
[39] K.V. Zakharchenko, A. Fasolino, J.H. Los and M.I. Katsnelson // *J. Phys.: Condens Matter* **23** (2011) 202202.